

A finite-difference model of atmospheric dynamics with the conservation laws

A.A. Fomenko and V.N. Krupchatnikov

A description of the basic model of atmosphere, which has been worked out in Siberian Scientific Hydrometeorological Institute and Computing Center of Siberian Division of Russian Academy of Sciences, is presented in this paper. Some conservations laws of the model allow to realize long-time integration. A limited-area variant of the model served as a basis of operative technology of regional weather prediction for Siberia. The results of predictions with this model are described at the end of this paper.

1. Introduction

In the present paper a basic atmospheric model is described. The variants of this model are intended for reproduction of climate and weather prediction. The possibility of long-time integration is provided with conservation of some invariants in finite-difference form, which exists in differential formulation of the task. Therefore in the statistical sense they allow to approach discrete model dynamics to the continuous atmospheric dynamics.

For short-range numerical weather prediction the demand in order to finite-difference scheme providing the fulfilment of integral properties may not be essential. In such case it is interesting to local accuracy of solution in the space and time. However, it is believed that supplementarily demands, which give realistic energy interaction between the waves of different scales may play here some positive role.

The experience of leading specialists (in particular ECMWF [13]) and the model author's experience were considered in this paper. We also took into account the availability of technical possibilities.

2. The basic equations

In the given model version Phillips' sigma-coordinate system is used, where

$$\sigma = \frac{p}{p_s},$$

p – pressure, p_s – its value on the Earth surface.

The basic system is

$$\begin{aligned} \frac{\partial u}{\partial t} - \frac{1}{\cos \varphi} Z p_s v \cos \varphi + \frac{1}{a \cos \varphi} \frac{\partial}{\partial \lambda} (\Phi + E) \\ + RT_v \frac{1}{a \cos \varphi} \frac{\partial \ln p_s}{\partial \lambda} + \dot{\sigma} \frac{\partial u}{\partial \sigma} = F_u, \end{aligned} \quad (2.1)$$

$$\frac{\partial v}{\partial t} + Z p_s u + \frac{1}{a} \frac{\partial}{\partial \varphi} (\Phi + E) + RT_v \frac{1}{a} \frac{\partial \ln p_s}{\partial \varphi} + \dot{\sigma} \frac{\partial v}{\partial \sigma} = F_v, \quad (2.2)$$

$$\frac{\partial T}{\partial t} + \frac{1}{p_s} \left[\frac{1}{a \cos \varphi} \left(p_s u \frac{\partial T}{\partial \lambda} + p_s v \cos \varphi \frac{\partial T}{\partial \varphi} \right) + p_s \dot{\sigma} \frac{\partial T}{\partial \sigma} - \frac{\kappa T_v \omega}{\sigma} \right] = Q, \quad (2.3)$$

$$\frac{\partial q}{\partial t} + \frac{1}{p_s} \left[\frac{1}{a \cos \varphi} \left(p_s u \frac{\partial q}{\partial \lambda} + p_s v \cos \varphi \frac{\partial q}{\partial \varphi} \right) + p_s \dot{\sigma} \frac{\partial q}{\partial \sigma} \right] = S, \quad (2.4)$$

$$\frac{\partial \Phi}{\partial \ln \sigma} = -RT_v, \quad (2.5)$$

$$\frac{\partial p_s}{\partial t} + \frac{1}{a \cos \varphi} \left[\frac{\partial}{\partial \lambda} (p_s u) + \frac{\partial}{\partial \varphi} (p_s v \cos \varphi) \right] + \frac{\partial}{\partial \sigma} (p_s \dot{\sigma}) = 0, \quad (2.6)$$

where

$$\omega = \frac{dp}{dt} = p_s \dot{\sigma} + \sigma \frac{\partial p_s}{\partial t} + \frac{\sigma}{a \cos \varphi} \left(p_s u \frac{\partial \ln p_s}{\partial \lambda} + p_s v \cos \varphi \frac{\partial \ln p_s}{\partial \varphi} \right).$$

We use the following notations:

$u, v, \dot{\sigma}$ – components of wind vector,

Φ – geopotential,

$T, T_v = (T + 0.607q)$ – temperature and virtual temperature,

q – specific humidity,

$Z = \frac{1}{p_s} \left[f + \frac{1}{a \cos \varphi} \left(\frac{\partial v}{\partial \lambda} - \frac{\partial u \cos \varphi}{\partial \varphi} \right) \right]$ – vertical component of potential
absolute vorticity,

f, a, λ, φ – the Coriolis parameter, Earth radius, longitude and latitude,

$E = \frac{1}{2}(u^2 + v^2)$ – kinetic energy,

$\kappa = \frac{R}{c_p}$, R – gas constant for dry air,

c_p – specific heat capacity for dry air at constant pressure,
 F_u, F_v, Q, S – nonadiabatic sources.

At the upper boundary of the atmosphere the natural boundary condition for the free surface is

$$(p_s \dot{\sigma})_{\sigma=0} = 0. \quad (2.7)$$

At the Earth surface we set the kinematic flow condition

$$(p_s \dot{\sigma})_{\sigma=1} = 0. \quad (2.8)$$

Besides that, the distribution of geopotential is

$$(\Phi)_{\sigma=1} = \Phi_s. \quad (2.9)$$

While passing to cartographic coordinates, the initial equation system may be presented in the following form

$$\frac{\partial}{\partial t}(mu) - Zmp_s v + m\dot{\sigma} \frac{\partial u}{\partial \sigma} + \frac{\partial}{\partial x}(E + \Phi) + RT_v \frac{\partial \ln p_s}{\partial x} = mF_u, \quad (2.10)$$

$$\frac{\partial}{\partial t}(m'v) + Zm'p_s u + m'\dot{\sigma} \frac{\partial v}{\partial \sigma} + \frac{\partial}{\partial y}(E + \Phi) + RT_v \frac{\partial \ln p_s}{\partial y} = m'F_v, \quad (2.11)$$

$$\frac{\partial}{\partial t}(mm'T) + \frac{u^*}{p_s} \frac{\partial T}{\partial x} + \frac{v^*}{p_s} \frac{\partial T}{\partial y} + mm'\dot{\sigma} \frac{\partial T}{\partial \sigma} - mm' \frac{\kappa T_v \omega}{p} = mm'Q, \quad (2.12)$$

$$\frac{\partial}{\partial t}(mm'q) + \frac{u^*}{p_s} \frac{\partial q}{\partial x} + \frac{v^*}{p_s} \frac{\partial q}{\partial y} + mm'\dot{\sigma} \frac{\partial q}{\partial \sigma} = mm'S, \quad (2.13)$$

$$\frac{\partial}{\partial t}(mm'p_s) + \frac{\partial u^*}{\partial x} + \frac{\partial v^*}{\partial y} + mm' \frac{\partial p_s \dot{\sigma}}{\partial \sigma} = 0, \quad (2.14)$$

$$\frac{\partial \Phi}{\partial \ln \sigma} = RT_v. \quad (2.15)$$

where

$$\begin{aligned} m &= a \cos \varphi \Delta \lambda, & m' &= a \Delta \varphi, \\ u^* &= m' p_s u, & v^* &= m p_s v, \\ x &= \lambda / \Delta \lambda, & y &= \varphi / \Delta \varphi. \end{aligned}$$

Such statement allows without difficulties to construct spatial-difference approximation [1], which gives the second order approximation and exhibits the potential enstrophy conservation law at the eddy advection by the horizontal velocity, and mass and energy conservation laws in adiabatic nondissipative processes [6].

3. Spatial-difference scheme

In the model Arakawa's *C*-grid is used. In the vertical direction the basic computational unequally-spaced levels are defined by the formulae

$$\sigma_k = 0.75s_k + 1.75s_k^3 - 1.5s_k^4,$$

where

$$s_k = (k - 1/2)/NLEV, \quad k = \overline{1, NLEV},$$

$NLEV$ is the number of vertical levels.

Let us introduce the notations

$$\pi_{i+1/2, j+1/2} = m_{j+1/2} m' (p_s)_{i+1/2, j+1/2}, \quad (3.1)$$

$$u^*_{i, j+1/2, k} = (\bar{p}_s^i u)_{i, j+1/2, k} m', \quad (3.2)$$

$$v^*_{i+1/2, j, k} = (\bar{p}_s^j v)_{i+1/2, j, k} m_j, \quad (3.3)$$

$$m_j = \frac{1}{2}(m_{j+1/2} + m_{j-1/2}), \quad (3.4)$$

where the overbar denotes the average with respect to corresponding variable. The equation for the surface pressure tendency, which is received by vertical integration of continuity equation, may be approximated by the following way

$$\frac{\partial}{\partial t} \pi_{i+1/2, j+1/2} + \sum_{k=1}^{NLEV} D_{i+1/2, j+1/2, k} \Delta \sigma_k = 0, \quad (3.5)$$

$$D_{i+1/2, j+1/2, k} = u^*_{i+1, j+1/2, k} - u^*_{i, j+1/2, k} + v^*_{i+1/2, j+1, k} - v^*_{i+1/2, j, k}. \quad (3.6)$$

Next, with the notations

$$\eta_{i, j, k} = \frac{1}{m_j m'} [m' v_{i+1/2, j, k} - m' v_{i-1/2, j, k} + (mu)_{i, j-1/2, k} - (mu)_{i, j+1/2, k}], \quad (3.7)$$

$$E_{i+1/2, j+1/2, k} = \frac{1}{m_{j+1/2}} \left(\frac{1}{2} \overline{mu^2}^i + \frac{1}{2} \overline{mv^2}^j \right)_{i+1/2, j+1/2, k}, \quad (3.8)$$

$$Z_{i, j, k} = \frac{2(f_j + \eta_{i, j, k})m_j}{m_{j+1/2}(\bar{p}_s^i)_{i, j+1/2} + m_{j-1/2}(\bar{p}_s^i)_{i, j-1/2}}, \quad (3.9)$$

the equations for horizontal components of wind may be written in the form

$$\begin{aligned}
\frac{\partial}{\partial t} m_{j+1/2} u_{i,j+1/2,k} &+ \varepsilon_{i+1/2,j+1/2,k} u_{i+1,j+1/2,k}^* - \varepsilon_{i-1/2,j+1/2,k} u_{i-1,j+1/2,k}^* \\
&- \alpha_{i,j+1/2,k} v_{i+1/2,j+1,k}^* - \beta_{i,j+1/2,k} v_{i-1/2,j+1,k}^* \\
&- \gamma_{i,j+1/2,k} v_{i-1/2,j,k}^* - \delta_{i,j+1/2,k} v_{i+1/2,j,k}^* \\
&+ \frac{m_{j+1/2}}{(\bar{p}_s)_{i,j+1/2}} \{[(\bar{p}_s \bar{\sigma}^i)_{i,j+1/2,k+1/2} (u_{i,j+1/2,k+1} - u_{i,j+1/2,k}) \\
&+ (\bar{p}_s \bar{\sigma}^i)_{i,j+1/2,k-1/2} (u_{i,j+1/2,k} - u_{i,j+1/2,k-1})]/(2\Delta\sigma_k)\} \\
&+ E_{i+1/2,j+1/2,k} - E_{i-1/2,j+1/2,k} \\
&+ \Phi_{i+1/2,j+1/2,k} - \Phi_{i-1/2,j+1/2,k} \\
&+ R\bar{T}_{i,j+1/2,k}^i [\ln(p_s)_{i+1/2,j+1/2} - \ln(p_s)_{i-1/2,j+1/2}] = m_{j+1/2} F_{u_{i,j+1/2,k}},
\end{aligned} \tag{3.10}$$

$$\begin{aligned}
\frac{\partial}{\partial t} m' v_{i+1/2,j,k} &+ \varphi_{i+1/2,j+1/2,k} v_{i+1/2,j+1,k}^* - \varphi_{i+1/2,j-1/2,k} v_{i+1/2,j-1,k}^* \\
&+ \gamma_{i+1,j+1/2,k} u_{i+1,j+1/2,k}^* + \delta_{i,j+1/2,k} u_{i,j+1/2,k}^* \\
&+ \alpha_{i,j-1/2,k} u_{i,j-1/2,k}^* + \beta_{i+1,j-1/2,k} u_{i+1,j-1/2,k}^* \\
&+ \frac{m'}{(\bar{p}_s)_{i+1/2,j}} \{[(\bar{p}_s \bar{\sigma}^j)_{i+1/2,j,k+1/2} (v_{i+1/2,j,k+1} - v_{i+1/2,j,k}) \\
&+ (\bar{p}_s \bar{\sigma}^j)_{i+1/2,j,k-1/2} (v_{i+1/2,j,k} - v_{i+1/2,j,k-1})]/(2\Delta\sigma_k)\} \\
&+ E_{i+1/2,j+1/2,k} - E_{i+1/2,j-1/2,k} \\
&+ \Phi_{i+1/2,j+1/2,k} - \Phi_{i+1/2,j-1/2,k} \\
&+ R\bar{T}_{i+1/2,j,k}^j [\ln(p_s)_{i+1/2,j+1/2} - \ln(p_s)_{i+1/2,j-1/2}] = m' F_{v_{i+1/2,j,k}},
\end{aligned} \tag{3.11}$$

where

$$\varphi_{i+1/2,j+1/2,k} = \frac{1}{24} (-Z_{i+1,j+1,k} + Z_{i,j+1,k} + Z_{i,j,k} - Z_{i+1,j,k}), \tag{3.12}$$

$$\varepsilon_{i+1/2,j+1/2,k} = \frac{1}{24} (Z_{i+1,j+1,k} + Z_{i,j+1,k} - Z_{i,j,k} - Z_{i+1,j,k}), \tag{3.13}$$

$$\alpha_{i,j+1/2,k} = \frac{1}{24} (2Z_{i+1,j+1,k} + Z_{i,j+1,k} + 2Z_{i,j,k} + Z_{i+1,j,k}), \tag{3.14}$$

$$\beta_{i,j+1/2,k} = \frac{1}{24} (Z_{i,j+1,k} + 2Z_{i-1,j+1,k} + Z_{i-1,j,k} + 2Z_{i,j,k}), \tag{3.15}$$

$$\gamma_{i,j+1/2,k} = \frac{1}{24} (2Z_{i,j+1,k} + Z_{i-1,j+1,k} + 2Z_{i-1,j,k} + Z_{i,j,k}), \tag{3.16}$$

$$\delta_{i,j+1/2,k} = \frac{1}{24} (Z_{i+1,j+1,k} + 2Z_{i,j+1,k} + Z_{i,j,k} + 2Z_{i+1,j,k}). \tag{3.17}$$

In so doing, with formal approximation of hydrostatic equation in the form

$$\Phi = \Phi_s + RGT_v,$$

where G is the upper-triangular matrix with the elements g_{lk} , ($g_{lk} = 0$, $l > k$), the consistent difference approximation of the expression $\frac{\kappa T_v \omega}{p}$ in the temperature equation, satisfying the energy conservation law, takes the form

$$\left(mm' \frac{\kappa T_v \omega}{p} \right)_k = \frac{\kappa (T_v)_k}{p_s} [V_k^* \cdot \nabla \ln p_s - (A \nabla V^*)_k],$$

where A is the lower-triangular matrix $a_{kl} = g_{lk} \frac{\Delta \sigma_l}{\Delta \sigma_k}$ (for simplicity the horizontal indexes are omitted).

The special choice of matrix G structure allows to construct an angular-momentum conserving scheme [10].

Therefore, spatial-difference approximation for the equation of temperature is

$$\begin{aligned} & \frac{\partial}{\partial t} m_{j+1/2} m' T_{i+1/2, j+1/2, k} \\ & + \frac{0.5}{(p_s)_{i+1/2, j+1/2}} [u_{i+1, j+1/2, k}^* (T_{i+3/2, j+1/2, k} - T_{i+1/2, j+1/2, k}) \\ & + u_{i, j+1/2, k}^* (T_{i+1/2, j+1/2, k} - T_{i-1/2, j+1/2, k}) \\ & + v_{i+1/2, j+1, k}^* (T_{i+1/2, j+3/2, k} - T_{i+1/2, j+1/2, k}) \\ & + v_{i+1/2, j, k}^* (T_{i+1/2, j+1/2, k} - T_{i+1/2, j-1/2, k})] \\ & + m_{j+1/2} m' [\dot{\sigma}_{i+1/2, j+1/2, k+1/2} (T_{i+1/2, j+1/2, k+1} - T_{i+1/2, j+1/2, k}) \\ & + \dot{\sigma}_{i+1/2, j+1/2, k-1/2} (T_{i+1/2, j+1/2, k} - T_{i+1/2, j+1/2, k-1})] / (2 \Delta \sigma_k) \\ & - m_{j+1/2} m' \left(\frac{\kappa T_v \omega}{p} \right)_{i+1/2, j+1/2, k} = m_{j+1/2} m' Q_{i+1/2, j+1/2, k}. \end{aligned} \quad (3.18)$$

The spatial-difference approximation for specific humidity equation is constructed in the same way.

The vertical component of the wind is calculated by the following diagnostic relationship, which is constructed from the continuity equation,

$$\begin{aligned} (p_s \dot{\sigma})_{i+1/2, j+1/2, k+1/2} &= \left(\sigma_{k+1/2} \sum_{l=1}^{NLEV} D_{i+1/2, j+1/2, l} \Delta \sigma_l \right. \\ & \left. - \sum_{l=1}^k D_{i+1/2, j+1/2, l} \Delta \sigma_l \right) / (m_{j+1/2} m'). \end{aligned} \quad (3.19)$$

It is not difficult to receive the modification of difference equations near the poles with the supposition $(v \cos \varphi)_p = 0$.

To eliminate the possibility of internal symmetric computational instability [5] the following modifications of finite-difference expressions (3.2), (3.3), (3.8) are foreseen

$$u^*_{i,j+1/2,k} = 0.25[(\bar{p}_s^i)_{i,j-1/2} + 2(\bar{p}_s^i)_{i,j+1/2} + (\bar{p}_s^i)_{i,j+3/2}]u_{i,j+1/2,k}m', \quad (3.20)$$

$$v^*_{i+1/2,j,k} = 0.25[(\bar{p}_s^j)_{i-1/2,j} + 2(\bar{p}_s^j)_{i+1/2,j} + (\bar{p}_s^j)_{i+3/2,j}]v_{i+1/2,j,k}m_j, \quad (3.21)$$

$$E_{i+1/2,j+1/2,k} = \frac{1}{8m_{j+1/2}} [(\overline{mu^2})_{i+1/2,j-1/2,k} + 2(\overline{mu^2})_{i+1/2,j+1/2,k} + (\overline{mu^2})_{i+1/2,j+3/2,k} + (\overline{mv^2})_{i-1/2,j+1/2,k} + 2(\overline{mv^2})_{i+1/2,j+1/2,k} + (\overline{mv^2})_{i+3/2,j+1/2,k}]. \quad (3.22)$$

4. The time integration scheme

The basis of time integration algorithms' construction is the semi-implicit scheme with respect to dynamical sources, the explicit scheme with respect to "slow" physical sources, and the implicit scheme with respect to "fast" physical sources (e.g. vertical diffusion).

The semi-implicit time integration scheme widely used in numerical prediction and general circulation models, belongs to the class of central time differences schemes and go ideologically back to G.I. Marchuk's [8] and A. Rober's [9] works. The basis of the method is that linear terms of dynamical part of numerical model, which are responsible for the gravitational waves evolution, are considered implicitly, while other terms – explicitly. Then our system in assumed indications takes the form

$$\delta_t \bar{u}^t + \frac{1}{m} \Delta_x \left(\frac{1}{2} \Delta_{tt} P \right) = A_u, \quad (4.1)$$

$$\delta_t \bar{v}^t + \frac{1}{m'} \Delta_y \left(\frac{1}{2} \Delta_{tt} P \right) = A_v, \quad (4.2)$$

$$\delta_t \bar{T}^t + A \left(\frac{1}{2} \Delta_{tt} d \right) = A_T, \quad (4.3)$$

$$\delta_t \overline{\ln p_s} + \Pi \cdot \left(\frac{1}{2} \Delta_{tt} d \right) = A_{p_s}. \quad (4.4)$$

Here the following property is used $\bar{X}^{2t} = X^t + \frac{1}{2} \Delta_{tt} X$.

$\Delta_{tt} = (\Delta_t)_t$, Δ_s , Δ_t – symmetrical differences by spatial and time respectively.

$\delta_t \bar{X}^t$ – central-differences time approximation,

A – the matrix of the divergency contribution into temperature tendency,

Π – row-vector with the elements $\Delta\sigma_k$,

$P = \Phi + RT_0 \ln p_s$, $d = \frac{1}{mm'}(\Delta_x m' u + \Delta_y m v)$,

u, v, d, T, P, Φ – column-vectors.

In so doing T_0 is column-vector of reference standard temperature, in the given model version it is not dependent on σ .

Let $B = GA + RT_0 \otimes \Pi$, then from (4.3) and (4.4) we have

$$\delta_t \bar{P}^t + B \left(\frac{1}{2} \Delta_{tt} d \right) = A_p, \quad (4.5)$$

and from (4.1) and (4.2)

$$\delta_t \bar{d}^t + \nabla^2 \left(\frac{1}{2} \Delta_{tt} P \right) = A_d, \quad (4.6)$$

where $A_u, A_v, A_T, A_{p_s}, A_P, A_d$ are the explicit tendencies.

Using the representation

$$\delta_t \bar{X}^t = \frac{1}{2\Delta t} \Delta_{tt} X + \frac{X^t - X^{t-1}}{\Delta t},$$

we transform (4.6) and (4.5) to

$$\frac{1}{2} \Delta_{tt} d + \Delta t \nabla^2 \left(\frac{1}{2} \Delta_{tt} P \right) = \Delta t A_d - (d^t - d^{t-1}), \quad (4.7)$$

$$\frac{1}{2} \Delta_{tt} P + \Delta t B \left(\frac{1}{2} \Delta_{tt} d \right) = \Delta t A_P - (P^t - P^{t-1}). \quad (4.8)$$

Let affect on (4.8) by operator $-\Delta t \nabla^2$, then we obtain the equation with respect to $\frac{1}{2} \Delta_{tt} d$

$$\begin{aligned} & \frac{1}{2} \Delta_{tt} d - \Delta t^2 \nabla^2 B \left(\frac{1}{2} \Delta_{tt} d \right) \\ &= \Delta t \left(A_d - \frac{d^t - d^{t-1}}{\Delta t} \right) - \Delta t^2 \nabla^2 \left(A_P - \frac{P^t - P^{t-1}}{\Delta t} \right). \end{aligned} \quad (4.9)$$

The $NLEV$ eigenvalues of the matrix B are squares of the phase speeds $C_{gk}^2 (k = 1, \dots, NLEV)$ of the models gravity waves in resting atmosphere. The vertical structure of the gravity waves are described by eigenfunctions $\zeta_k (k = 1, \dots, NLEV)$. The system may be transformed, using the matrix

$$E = (\zeta_1, \dots, \zeta_{NLEV}). \quad (4.10)$$

We define the vector Y by formulae

$$Y = E^{-1} \left(\frac{1}{2} \Delta_{tt} d \right), \quad (4.11)$$

and using the fact that

$$E^{-1} B E = \text{diag}(C_{gk}^2), \quad (4.12)$$

we give the *NLEV* equations

$$Y_k - \Delta t^2 C_{gk}^2 \nabla^2 Y_k = E^{-1} (\text{rhs}(4.9)), \quad (4.13)$$

where $\text{rhs}(4.9)$ is the right side of (4.9).

The polar boundary conditions for equation (4.13) may be derived from this equation using Green's formulae for polar cups. In the solving of (4.13) one of the variants of direct method of partial reduction with the Fourier transform was used.

In the regional model version the poles are assumed not to belong to the calculation forecast region. In this case, solving the equation (4.13), we set the uniform Dirichlet conditions at the regional boundary. The matrix of general equation system passes the diagonal predominance and hence is non-singular. In regional model version the method of boundary conditions assimilation, which is the modification of relaxation method, developed in [2], is used.

In order to overcome some stability restrictions arising from the convergence of the meridians to poles, a latitudinal dependent spatial filtering operator can be applied to all tendencies.

5. Sub-grid scale processes

In the given model version we use the linear horizontal second-order diffusion scheme, though, there are variants of linear and nonlinear fourth-order schemes.

The calculation of surface flows is based on the Monin-Obukhov similarity theory, where wind and temperature profiles depend on outer parameters and on surface moment and heat flows. Equations used in the model for moment, sensible heat and moisture flows are different for stably and unstably stratified surface level. Earth surface roughness height Z_0 over the sea is calculated with the help of ratio

$$Z_0 = 0.032 \frac{u_*^2}{g}.$$

it is assumed that $Z_0 \geq 0.0015$ cm. Over the land Z_0 is assumed to depend on vegetation amount, urbanization and topography height and variability in accordance with [12]. Over the ice Z_0 is taken as 0.0015 m.

Flows over the surface layer are calculated on the basis of mixing length theory, where diffusion factors are defined in different ways for stable and unstable stratifications.

Before the calculation of main variables at each step the general convective adjustment is performed breaking up into several stages:

- exclusion of negative values in the moisture field;
- performing of dry convective adjustment;
- moist convection.

For the exclusion of negative values of the moisture field, which can occur due to the truncation errors of central difference scheme simultaneously with condensation processes, the scheme which retains the total moisture content is used.

The deep moisture convection parameterization scheme is based on Kuo's [7] method, in which the following assumptions were used:

- a criterion for the convection existence is the presence of moisture convergence at lower levels and conditionally unstable stratification in the lower troposphere,
- the rise of air in clouds is performed pseudoadiabatically, the upper cloud boundary is located at the level, where the cloud temperature equals the ambient air temperature,
- forming clouds get mixed up instantly with ambient air.

The main distinction of the used scheme from Kuo's parameterization is that not only convective clouds, generated by air rise from the Earth surface, are considered, but also clouds being conceived at higher levels, where moisture convergence also can occur.

In the non-convective cloudiness parameterization scheme the condensation process occurs when specific humidity reaches the saturation value, but liquid water does not fall in the form of precipitation until one of two conditions will be fulfilled.

The first condition, a fairly cold cloud top is based on the mechanism which takes into account that ice nuclei generation goes more effectively when temperature is below some threshold temperature T_c . After nuclei generation their fast growth due to overcooled water drops and precipitation fall-out follow.

The second condition, a fairly thick cloud is based on the fact that the rain drop coagulation increases when these drops number density increases. In this case criterion is that cloud water must exceed some value.

Sea temperature is treated as assigned. This assumption is made both for open water and for water covered by ice.

At the land the thin soil layer is signed out with certain heat capacity, which exchanges heat and moisture with atmosphere and deep soil (active soil layer).

The snow melting is considered each time when snow presents and land temperature exceeds ice melting temperature. In this case land temperature is taken equal the ice melting temperature, while incoming energy goes to the snow melting.

Moisture over the sea is equal to the saturation value at given temperature.

Soil moisture and snow cover are calculated with account of precipitation, evaporation, melt water, run-off and moisture diffusion into soil.

The solution of the radiative transfer equation to obtain the fluxes is very expensive, and we do it only twice a day at every grid point. When the diurnal cycle is explicitly considered in solar flux, we have to perform the full radiation computation more than twice a day at coarser grid.

The solution of the radiative transfer equation involves integrations over angles, over vertical coordinate and over some intervals of spectrum. We suppose that we can separate the whole spectrum into two intervals: short waves ($B_\nu(T) = 0$) and long waves ($S_{ov} = 0$). In order to avoid a huge number of computations at different frequencies, we have to find how to determine optical depth ν , single-scattering albedo ω and phase function [3].

The solution of the monochromatic equation being of exponential type, the problem comes from the nonlinear nature of the exponential functions, and we have to use spectrally averaged coefficients of absorption and scattering only when the coefficients have the same order of magnitude throughout the considered spectral interval. This is a case for cloud-aerosols absorption and scattering and Rayleigh scattering (for short waves) in some spectrum domains (3 for long waves, 2 for short waves) and we have grey effects except for gaseous absorption in these intervals. An extra difficulty arises in the case of gaseous absorption (CO_2 , H_2O , O_3), because the coefficients strongly depend on temperature and pressure.

We, therefore, use empirical transmission functions for gases. First of all we make computation without any gaseous absorption, the resulting flux represents either the parallel flux or the upward or downward diffuse flux. After that we add each gas H_2O , CO_2 , O_3 with small absorption

coefficient and finally we compute the real flux. In the long wave domain of the spectrum the problem is more complicated, because there is not a single external source and every absorption is accompanied by an equivalent emission. Hence, to estimate the amounts of absorbers we have to compare computations with and without gases in an isothermal case.

To resolve the vertical integration problem, we suppose that each layer is vertically homogeneous absorbing and scattering medium, and that in each spectral interval of the long wave domain the Planck function vary linearly with the optical depth through every layer. We use the two-stream Eddington approximation. At each level both upward and downward diffuse radiation fields are hemispherically isotropic. The radiation model uses the cloud prediction scheme which allows for four cloud type – convective and three layer clouds (high, middle, low level) [11].

6. Verification of operational forecasts

In this section the results of operative using of regional version of the model are presented. Operative predictions are doing one time/day with meteorological data of 12h GMT for Siberian region during 60 hours. The domain of forecast is in the form $1.66^\circ \times 1.25^\circ$ longitude-latitude grids covering the region from $40^\circ - 146.6^\circ E$ and $40^\circ - 80^\circ N$. Initial fields are received as a result of two-dimension one-element objective analysis by optimal interpolation method. The first-guess is the 12h forecast with this model. The using of the procedure of nonlinear normal mode initialization is given initial consistent fields of temperature and wind.

Boundary conditions are received from the prediction geopotential data of NMC, which are provided by connection canals in the GRID's code. Maximum accessible data quantity are only five izobaric levels 100, 300, 500, 850, 1000 mb with discrete in 12h. Prediction data are interpolated with respect to vertical on all levels. The temperature is reconstructed by geopotential, horizontal wind components are geostrophical. Because we have no data upper 100 mb, the izothermal distribution of temperature is supposed. Linear interpolation by time is used for boundary conditions inside 12h intervals.

It is necessary to note that the GRID's information data give the possibility, as a rule, to use changing by time boundary conditions only for 36h forecast. After that the stationary boundary conditions are used.

In spite of coarse boundary conditions, which are connected with the unsufficient quantity of external prediction informations, the quality of predictions is quite satisfactory, although less than with using boundary condi-

tions with whole volume.

In Figure 1 tendency correlations of 500 mb geopotential and surface pressure 24 and 48 hours forecasts in 1992 year are demonstrated.

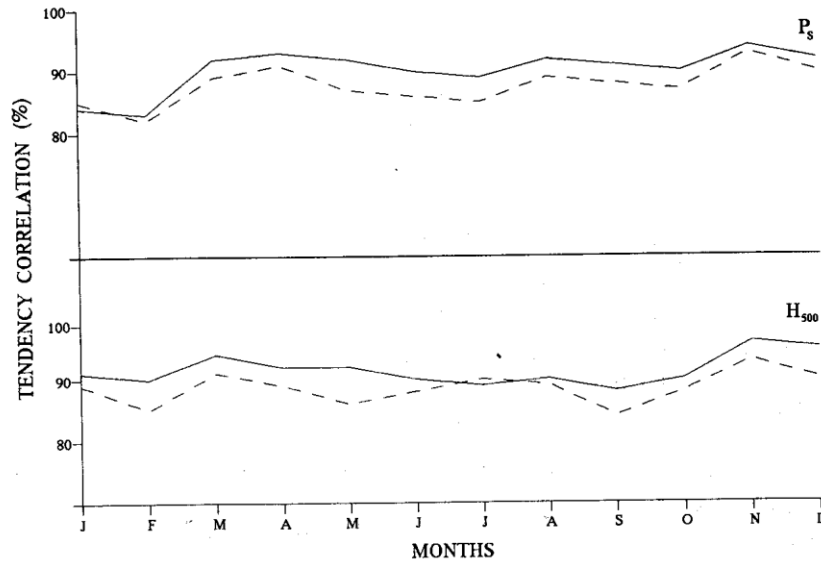


Figure 1. Tendency correlation coefficients for surface pressure p_s (top) and 500 gPa heights H_{500} (bottom) averaged over region for 24h (solid line) and 48h (dashed line) forecasts in 1992 year

Figure 2 demonstrates the possibilities of predictability of the model. It is evident that the utility of predictions is more than 60h.

7. Conclusion

In this paper we introduced the basic model of atmosphere. At present the limited-area version of this model is used for operative numerical weather prediction in Siberian region. Estimations of weather predictions, which were got by the means of model, show a good quality. Global version of the model is intended for climatic investigations. Interaction between limited-area and global models will allow to carry out numerical experiments on study of influence of global climatic changes on to regional scales.

This work has been supported financially by Soros Fund.

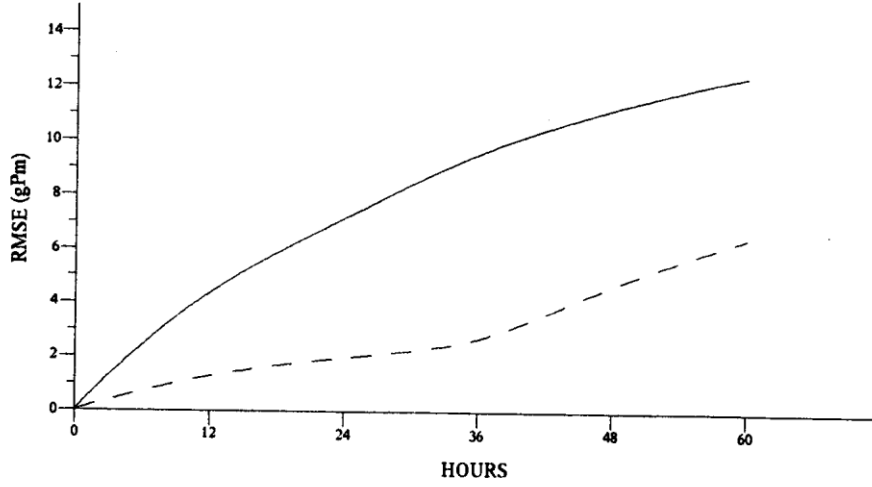


Figure 2. January 1993 year root mean square errors of forecast (dashed line) and persistence (solid line) for 500 gPa heights

Appendix

The pre and post-processing package provides an interface between the model and databases for dissemination and archiving. After some comparison of numerical experiments the next procedures were applied. Cubic tension splines with the vertical coordinate $\ln p$ were used for the interpolation in the vertical from the model coordinates to constant pressure levels and back. Preliminarily the specific humidity was transformed to the terms of relative humidity.

Surface pressure p_s was calculated from the mean sea-level pressure p_{msl} by the means of some modification of the Shuman-Hovermaile[4] scheme.

For the calculation mean sea-level pressure p_{msl} from p_s the following procedure was used.

Define

$$T_s = T_{NLEV} + \gamma(\Phi_{NLEV} - \Phi_s)/g,$$

$$T_0 = T_s + \gamma\Phi_s/g,$$

$$T_m = \begin{cases} T_0 & \text{at } T_0 \leq 290.5, \\ 290.5 - 0.005(T_0 - 290.5)^2 & \text{at } T_0 > 290.5, T_s > 290.5, \\ 290.5 & \text{in other cases,} \end{cases}$$

and

$$T_g = 0.5(T_m + T_s).$$

After that

$$p_{msl} = p_s \exp(\Phi_s / RT_g).$$

T_{1000} was obtained from T_{NLEV} by means of using standard profile of temperature.

References

- [1] A. Arakawa, V.R. Lamb, A potential enstrophy and energy conserving scheme for shallow-water equations, MWR, Vol. 109, 1981, 11-26.
- [2] H.C. Davies, A lateral boundary formulation for multi-level prediction model, Quart. J. Roy. Meteorol. Soc., Vol. 102, 1976, 405-418.
- [3] J.-F. Geleyn, A. Hollingsworth, An economical analytical method for the computation of the interaction between scattering and line absorption of radiation, Beitr. Phys. Atmosph., Vol. 52, 1979, 1-16.
- [4] G.F. Gerrity, The LFM model - 1976: A documentation, NOAA Tech. Memorandum, 1977.
- [5] A. Hollingsworth et al., An internal symmetric computational instability, Quart. J. Roy. Meteorol. Soc., Vol. 109, 1983, 417-428.
- [6] V.N. Krupchatnikov, V.K. Maev, A.A. Fomenko, A model of the atmosphere on a limited area with high resolution, Izv. AN SSSR, FAO, 28, No. 1, 1992, 33-45 (In Russian).
- [7] H.L. Kuo, Further studies of the parameterization of the influence of cumulus convection in large-scale flow, J. Atm. Sci., Vol. 31, 1974, 1232-1240.
- [8] G.I. Marchuk, Numerical Methods in Weather Prediction, Gidrometeoizdat, Leningrad, 1967, (Translated from Russian, A. Arakawa and Y. Mintz, eds., Academic Press, New York, 1974).
- [9] A.J. Robert, The integration of a spectral model of the atmosphere by the implicit method, Proc.WMO/IUGG Symposium of Numerical Weather Prediction in Tokio, 1968, Meteor. Soc. Japan, 1969, VII-19-VII-24.
- [10] A.J. Simmons, D.M. Burridge, An energy and angular-momentum conserving vertical finite-difference scheme and hybrid vertical coordinates, MWR, Vol. 109, 1981, 758-766.
- [11] J.M. Slingo, The development and verification of a cloud prediction scheme for the ECMWF model, Quart. J. Roy. Meteorol. Soc., Vol. 113, 1987, 899-928.
- [12] S. Tibaldi, J.-F. Geleyn, The production of a new orography, land-sea mask and associated climatological surface fields for operational purposes, ECMWF Tech. Memo., No. 40, 1981.
- [13] M. Tiedtke, J.-F. Geleyn, A. Hollingsworth, J.-F. Lois, ECMWF model-parameterization of sub-grid scale processes, ECMWF Tech. Rep., No. 10, 1979.